

## Structure of the Galaxies of the NGC 80 Group: Two-Tiered Disks

M. A. Startseva<sup>1</sup>, O. K. Sil'chenko<sup>1</sup>, and A. V. Moiseev<sup>2</sup>

<sup>1</sup>*Sternberg Astronomical Institute, Moscow State University, Moscow, Russia*

<sup>2</sup>*Special Astrophysical Observatory, Russian Academy of Sciences,  
Nizhnii Arkhyz, Karachaevo-Cherkessia Republic, Russia*

Received March 20, 2009; in final form, June 25, 2009

**Abstract**—Two-color photometric data obtained on the 6-m telescope of the Special Astrophysical Observatory are used to analyze the structure of 13 large disk galaxies in the NGC 80 group. Nine of the 13 studied galaxies are classified as lenticular galaxies. The stellar populations in the galaxies are very diverse, from old stars with ages of  $T > 10$  billion years (IC 1541) to relatively young stars with ages of  $T \sim 1\text{--}3$  billion years (IC 1548, NGC 85); in one case, star formation is ongoing (UCM 0018+2216). In most of the studied galaxies, more precisely in all of them brighter than  $M_B \sim -18$ , two-tiered stellar disks are detected, whose radial surface-brightness profiles can be described by two exponential segments with different characteristic scales—shorter near the center and longer at the periphery. All of the dwarf S0 galaxies with single-tiered disks are close companions to larger galaxies. Except for this fact, no dependence of the properties of S0 galaxies on distance from the center of the group is found. Morphological signs of a “minor merger” are found in the lenticular galaxy NGC 85. Based on these last two results, it is concluded that the most probable mechanism for their transformation of spiral into lenticular galaxies in groups is gravitational (minor mergers and tidal interactions).

PACS numbers: 98.52.Nr, 98.62.Ai, 98.62.Lv, 98.65.At, 95.85.Kr

DOI: 10.1134/S1063772909120038

### 1. INTRODUCTION

It is currently believed that lenticular galaxies, which Hubble [1] took to be intermediate between elliptical and spiral galaxies, have morphologically formed in the past five billion years which is confirmed by observations of clusters and groups at intermediate redshifts,  $z = 0.2\text{--}0.7$  [2, 3]. This picture is no longer doubted. However, the diversity of opinions and results grows sharply in connection with details and specific mechanisms for the transformation of spiral into lenticular galaxies. It is clear that, in order to transform a spiral into a lenticular galaxy, star formation must cease and the stellar disk must be dynamically heated, to allow the dissipation of the spiral arms. However, it is not obvious whether it is sufficient simply to cease star formation or whether it is necessary to sharply (and briefly) increase the intensity and efficiency of star formation at the galactic center to facilitate the growth of the bulge, which is, on average, more prominent in lenticulars than in spirals of the same mass [4, 5]. There is currently no observational answer to this question, but distinguishing the “mechanism” leading to the transformation of a spiral into an S0 galaxy depends on this answer. If we consider gas-dynamical mechanisms, the frontal (dynamical) pressure of the hot intergalactic medium

due to the speed with which the galaxy moves relative to the medium will predominantly “sweep out” gas from the galaxy, emptying it of “fuel” for star formation [6], while the static pressure of the surrounding hot gas will “squeeze” the cool gas of the galactic disk, stimulating star formation [7]. As a rule, gravitational effects, such as tidal perturbation of the disk dynamics by the gravitation of the cluster (group) as a whole or pair interactions between galaxies, primarily lead to the formation of a central bar, with the bar then facilitating the radial flow of gas in the disk toward the galactic center, intensifying star formation there. The outer parts of stellar disks that are left without gas in this way are dynamically heated, and can no longer support spiral structure [8–10]. Tidal effects also “strip” gas from the peripheries of galactic disks.

Just as the dominant mechanism for the transformation of spiral into lenticular galaxies is unclear, it is likewise not clear where this transformation occurs. At  $z = 0$ , the highest density of lenticular galaxies is in clusters, where they comprise up to 60% of all cluster galaxies [11, 12]. This suggests that the transformation itself occurs in clusters [2, 13], especially since the gas-dynamical conditions (a dense, hot intergalactic medium, a high velocity dispersion for the galaxies) are favorable for this. However, the idea

that lenticular galaxies are mainly formed in groups has gained more and more support in recent years; in this picture, groups accreting into clusters bring with them already formed lenticular galaxies [3]. This view is based on the observed morphological “mix” of galaxies in various types of environments at  $z = 0.3\text{--}0.7$ . If this picture is correct, it immediately identifies gravitational pair interactions, especially “minor mergers”—the absorption of small satellites—as the most likely mechanism for the formation of S0 galaxies, since groups differ from clusters primarily in the lower velocity dispersions for their member galaxies, which reduces the action of gas-dynamical effects, while enhancing the action of gravitational effects. The properties of galaxies in groups are currently known substantially less well than the properties of galaxies in clusters, making studies of the structure and stellar populations of lenticular galaxies in groups topical and of key importance for our further understanding of galaxy formation.

In the current study,<sup>1</sup> we consider the structure of lenticular galaxies, as well as early-type spiral galaxies, which are the most likely candidates for pre-lenticular galaxies, in the massive X-ray group NGC 80. NGC 80 is also known as GH3 [14], SRGb063 [15], and U013 [16], and is sometimes classified as a “poor cluster” (WBL 009 [17]). The X-ray flux from NGC 80 is  $\log L_X(h_{100}^{-2} \text{ erg/s}) = 42.56 \pm 0.09$  [15], which is average for rich groups, and its estimated mass exceeds  $10^{14} M_\odot$  [16]. The group occupies nearly a degree on the sky; our recent paper [18] shows a portion of a Palomar map  $45'$  in size that contains nearly all the large group members. Radial velocity measurements were used to distinguish 45 group members in [19]; our visual examination of the maps indicates that at least half of these (24 galaxies) are late-type spiral galaxies, which is surprising, given the powerful X-ray halo of the group (it is thought that a hot, intergalactic medium is possessed by groups populated primarily by early-type galaxies). Could it be that NGC 80 is a young group, so that the process of transforming spiral group members into lenticulars has not yet finished? To investigate the properties of a sample of lenticular galaxies in this group, we obtained images in the  $B$  and  $V$  filters for fields around five large galaxies studied by us earlier in [18], and carried out surface photometry of objects with radii exceeding  $10''$ . A list of studied galaxies is presented in Table 1 together with their global characteristics.

<sup>1</sup> This study is based on the results of observations on the 6-m telescope of the Special Astrophysical Observatory of the Russian Academy of Sciences.

## 2. OBSERVATIONS

Photometric data were obtained on the 6-m telescope of the Special Astrophysical Observatory of the Russian Academy of Sciences using the SCORPIO instrument [20] in a direct-imaging regime. The receiver was a  $2048 \times 2048$  EEV 42-40 CCD array. The counts were obtained in a double-pixel mode, which provided a scale of  $0.35''$  per pixel. The total field of view was  $6.1'$ . The observations were carried out in the standard Johnson  $B$  and  $V$  filters. An exposure of a dawn sky was taken for flat-fielding.

A detailed journal of observations is presented in Table 2. The observations of the group NGC 80 were conducted on August 21, 2007 under photometric conditions, and the seeing was roughly  $2''$ . We took exposures of five fields centered on the bright galaxies NGC 80, NGC 86, NGC 93, IC 1548, and IC 1541. The galaxy NGC 80 was used as a photometric standard; a good set of aperture photoelectric-photometry data are available for this galaxy in the HYPERLEDA database, primarily from [21].

In addition to the photometric data, we analyzed a series of spectral observations. The central region of NGC 85 was observed with the MPFS integral-field spectrograph of the 6-m telescope in September 2008 at blue-green wavelengths,  $4150\text{--}5650 \text{ \AA}$ , with an inverse dispersion of  $0.75 \text{ \AA/pixel}$  (a spectral resolution of about  $3.5 \text{ \AA}$ ) (for a description of this instrument, see [22]). The receiver for these observations was the same  $2048 \times 2048$  CCD array. In the MPFS observations, a  $16 \times 16$  microlens set constructs a pupil array, whose signals are provided to the entrance of the diffraction spectrograph. This configuration enables the simultaneous recording of 256 spectra, each of which corresponds to a spatial element of the galaxy image  $1.0'' \times 1.0''$  in size; accordingly, the MPFS field of view is  $16'' \times 16''$ . The data were used to investigate the rotation of the stellar component (we were not able to detect ionized gas in NGC 85), via a cross correlation between the galaxy spectra and MPFS data for K giant stars observed on the same night. The age and chemical composition of the stellar population in the nucleus and circum-nuclear region were estimated by determining the Lick  $H\beta$ , Mgb, Fe5270, and Fe5335 indices [23] and comparing them with the models for “simple” stellar populations of Thomas et al. [24].

To study kinematics at distances of more than  $8''$  from the center, the lenticular galaxy IC 1541 at the periphery of the group was observed on September 2, 2008 with the SCORPIO reductor in a long-slit regime. The slit orientation was close to that of the major axis of the galaxy. The exposure was 30 min, and the VPHG1200R “red” grism was used,

**Table 1.** Global parameters of the studied galaxies

Number <sup>1</sup>	Alternate name	Type (NED <sup>2</sup> )	$D_{25}$ (LED <sup>3</sup> )	$M_B$ (LED <sup>3</sup> )	$(B - V)_{3''}^4$	$V_r$ , km/s (NED <sup>2</sup> )	$\Delta$ , Mpc <sup>1</sup>
—	NGC 80	SA0—	1.82'	−21.6	1.03	5698	~0
029	—	—	0.36	−17.6	0.84	5709	0.117
030	—	—	0.33	−17.9	0.95	6035	0.132
034	NGC 81	—	0.41	−18.8	0.99	6130	0.097
035	—	—	0.33 <sup>4</sup>	−18 <sup>4</sup>	0.96	5372	0.111
040	NGC 85	S0	0.68	−19.5	1.18	6204	0.115
016	IC 1541	S0	0.72	−19.4	1.04	5926	0.544
055	IC 1548	S0	0.68	−19.3	1.00	5746	0.400
058	NGC 93	S (Sb) <sup>3</sup>	1.32	−20.8	1.06	5380	0.096
041	NGC 86	Sbc (S0/a) <sup>3</sup>	0.74	−20.0	1.05	5591	0.153
044	MCG 04-02-010	S (Sbc) <sup>3</sup>	0.89	−20.3	1.17	6630	0.185
051	CGCG 479-014B	Sc	0.63	−18.5	0.93	5850	0.377
—	UCM 0018+2216	Sb	0.29	−17.3	0.72	5066	0.14

<sup>1</sup> According to the catalog [19]; from this same source, the distance to the group is 77 Mpc.

<sup>2</sup> NASA/IPAC Extragalactic Database.

<sup>3</sup> Lyon–Meudon Extragalactic Database.

<sup>4</sup> Current study.

**Table 2.** Photometric and spectral observations of galaxies of the group in 2007–2008

NGC/IC	Observation date	Instrument	Wavelength range	Exposure, s	Spatial resolution
80	21.08.2007	SCORPIO/IM	$V$	60	2.3''
80	21.08.2007	SCORPIO/IM	$B$	180	2.1
93	21.08.2007	SCORPIO/IM	$B$	180 × 2	2.0
93	21.08.2007	SCORPIO/IM	$V$	60 × 3	2.0
86	21.08.2007	SCORPIO/IM	$V$	120 × 2	2.2
86	21.08.2007	SCORPIO/IM	$B$	180 × 3	2.0
1548	21.08.2007	SCORPIO/IM	$V$	120 × 2	1.9
1548	21.08.2007	SCORPIO/IM	$B$	180 × 3	2.1
1541	21.08.2007	SCORPIO/IM	$B$	180 × 3	1.8
1541	21.08.2007	SCORPIO/IM	$V$	90 × 3	2.3
85	04.09.2008	MPFS	4200–5600 Å	5400	1.9
1541	02.09.2008	SCORPIO/LS	5700–7400 Å	1800	2.3

providing wavelengths 5700–7400 Å and a spectral resolution of about 5 Å, since the original goal was to search for weak emission from ionized gas in IC 1541. However, no traces of emission were detected, and the data were instead used to construct line-of-sight

velocity cross-section for the stellar component (a rotation curve) via cross correlation of the galaxy spectra at various distances from the center and spectra of the twilight sky taken the same night with the same grid.

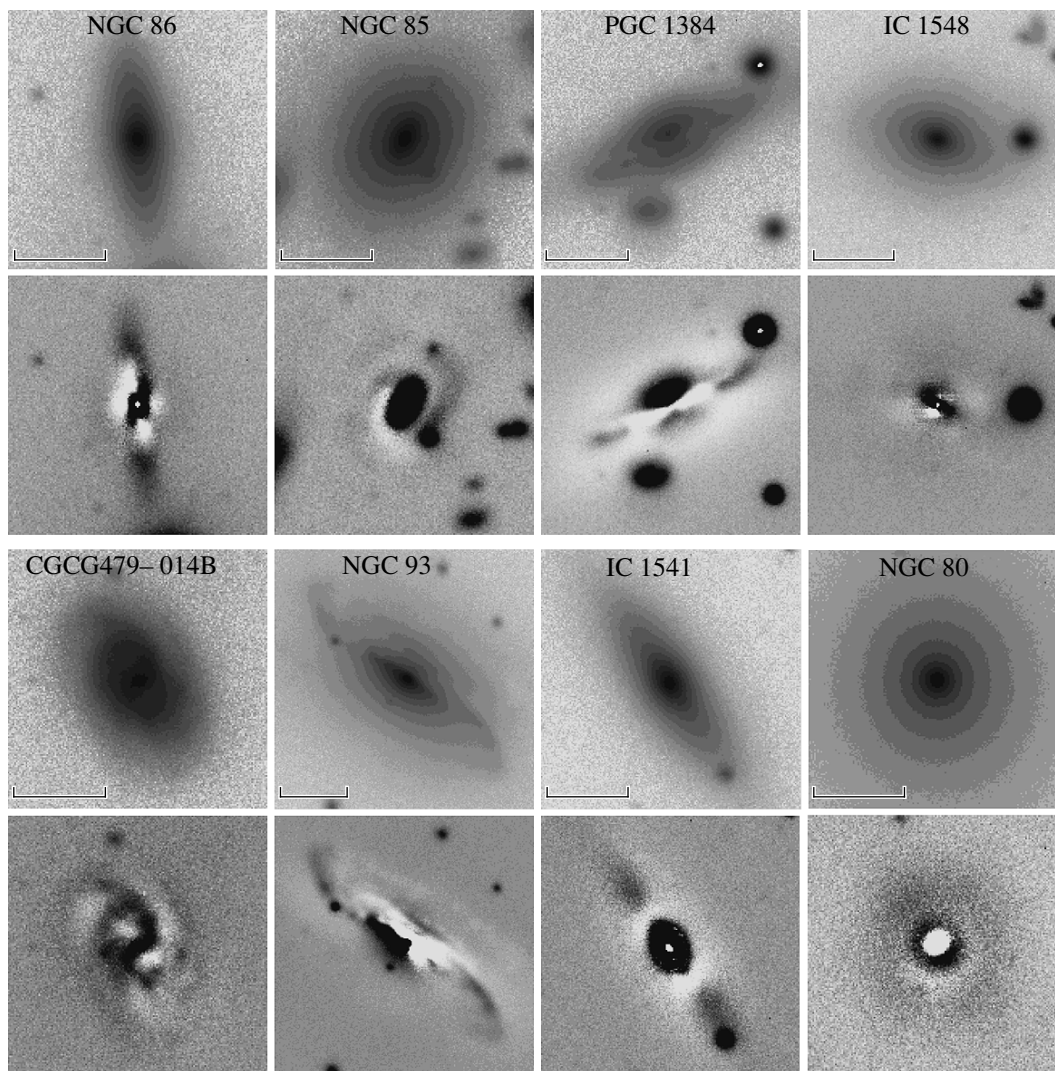


**Fig. 1.** Original images obtained with the SCORPIO reductor in the  $V$  filter for eight large group members (the first and third horizontal rows show images with headers; the intensity scale is logarithmic) and maps of the residual brightness after subtracting multi-tier models for the images (the second and fourth horizontal rows show these maps beneath the corresponding original maps; the intensity scale is linear). The scale for the section is  $20''$ .

### 3. ANALYSIS OF THE STRUCTURE OF DISK GALAXIES IN THE NGC 80 GROUP

We carried out a decomposition of the  $B$  and  $V$  radial surface-brightness profiles of the studied galaxies. Figures 1 and 2 present the original  $V$  images of the galaxies, together with the residual brightnesses after subtracting our models.

The decomposition was carried out using the interactive GIDRA program, which realizes a method for successively constructing one-dimensional profiles and two-dimensional models (see, for example, [25]). The main idea of the method is to construct radial dependences for the surface brightness averaged in elliptical rings. The shape of these elliptical rings (position angle, major axis, and axial ratio) was specified based on an isophotal analysis of

the images conducted using the program FITELL of V.V. Vlasyuk. Images of foreground stars projected onto the galaxy were either masked or removed by subtracting a symmetrical profile corresponding to the scattering function for a point source (the case of a bright star next to NGC 86). Further, having constructed the azimuthally averaged surface-brightness profiles, the GIDRA program derived a piece-wise approximation using a Sérsic law [26]:

$$\mu(r) = \mu_e + 1.086b_n[(r/r_e)^{\frac{1}{n}} - 1],$$

where  $n$ ,  $r_e$ , and  $\mu_e$  are parameters of the model and  $b_n \approx 2n - 0.32$ . We distinguished structural components of the galaxy, beginning with the outer regions, which we assumed to be disks with exponential brightness profiles [27]—a special case of a Sérsic law

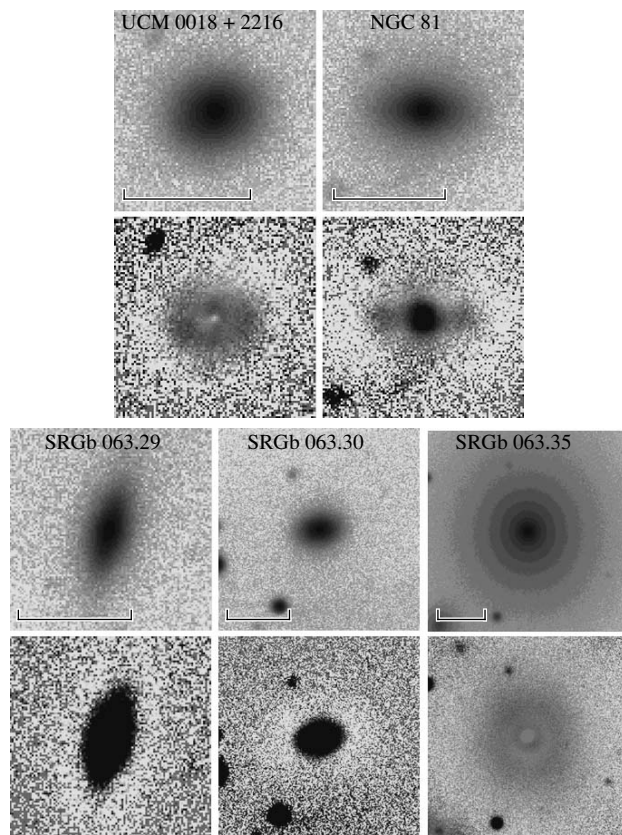


**Fig. 2.** Same as Fig. 1 for five dwarf group members. The residual brightness is given on a logarithmic intensity scale.

with  $n = 1$ . Having fit an exponential to the brightness profile of the outer stellar disk and determined its parameters, we constructed a two-dimensional model and subtracted it from the observed galaxy image. Further, the procedure of constructing and fitting an azimuthally averaged surface-brightness profile was repeated. If the ellipticity of the residual isophotes was not very different from the ellipticity of the outer isophotes, we concluded that a separate inner stellar disk was present in the galaxy, and fit it using a separate exponential law. After subtracting this inner disk, there usually remained a central bulge, for which the Sérsic parameter  $n$  was varied rather than fixed. However, in most cases, we obtained an exponential brightness profile for the bulge as well. This is the first conclusion of our analysis of the structure of early-type disk galaxies in the NGC 80 group: most of them have exponential bulges. An example of decomposing the brightness profile for a giant lenticular galaxy (IC 1541 at the periphery of the group) into two disks and an exponential bulge is shown in Fig. 3a. This galaxy is oriented nearly edge-on, and a thickening associated with the bulge is visible by eye only in the very central region of the galaxy; the two stellar disks with different exponential scales have comparable thicknesses. Figure 3a shows how

deep our photometry is: the galactic disk extends to a radius of 30 kpc and the limiting surface brightness of  $\mu_V = 27.7^m/\text{arcsec}^2$  extends appreciably beyond the Holmberg radius.

The parameters of the photometric models for the sample galaxies are presented in Table 3, which gives the central surface brightness  $\mu_0 = \mu(0)$ , **not** reduced to a face-on orientation. All the large lenticular galaxies have two-tiered exponential disks and exponential bulges. The bulge of NGC 93 is best fit with a Sérsic law with an index of two, as is typical for giant Sb galaxies. An interesting feature is shown by dwarf lenticular galaxies that are satellites of the central galaxy of the NGC 80 group: three of four display a single stellar disk and, when present, the central spheroid is best fit with a Sérsic law with index  $n < 1$ , as is typical for dwarf “diffuse” spheroidal galaxies. In one case—namely the nearest close companion to NGC 80, SRGb063.035—there is no bulge, and the entire galaxy consists of a single disk (Fig. 3b). Stellar structure with very low surface brightness is also visible around the single exponential disk of a close companion to NGC 86—UCM 0018+2216, which is an Sb galaxy according to the NED classification; however, no spiral arms are visible in the disk of UCM 0018+2216 in our plots and we re-classify

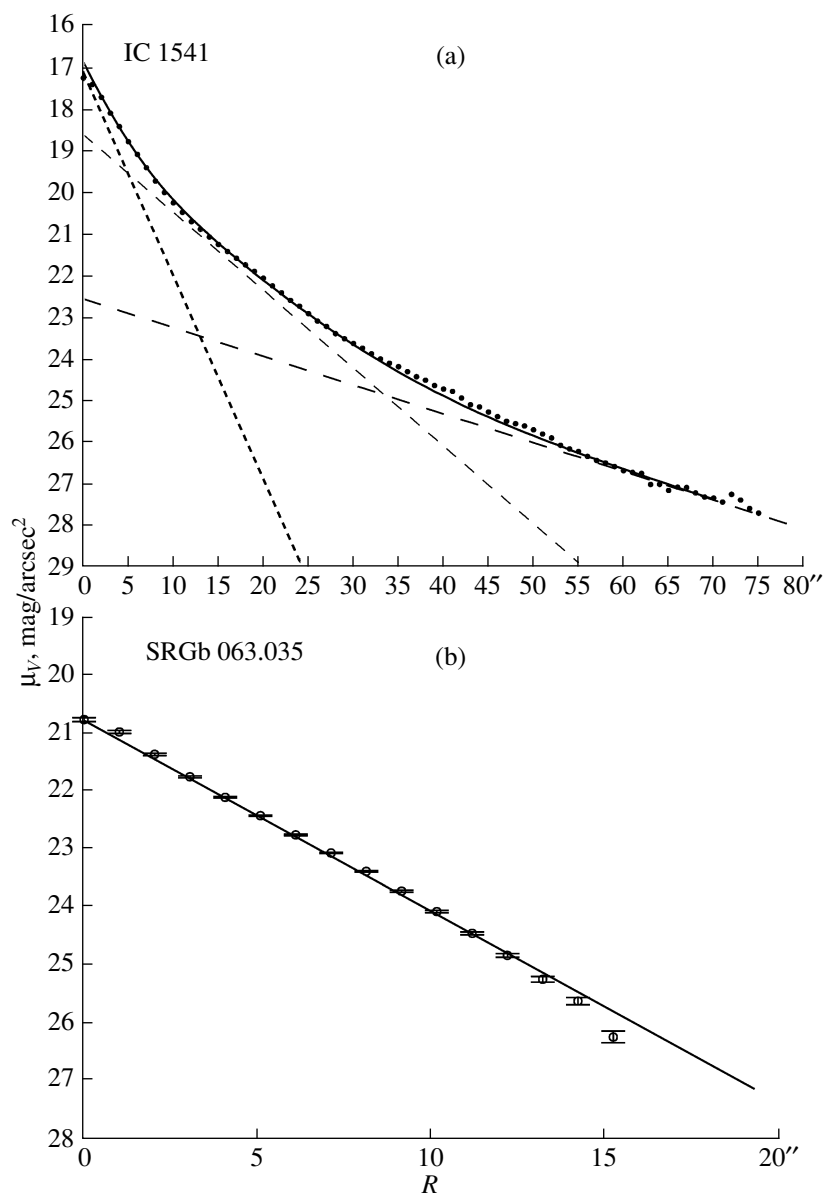


**Fig. 3.** Examples of separating a surface-brightness profile (in  $V$ ) into components. (a) The lenticular galaxy IC 1541. The long-dashed curve shows results for the outer stellar disk, the short-dashed curve results for the inner stellar disk, and the dotted curve results for the pseudobulge. The points represent the observational data: surface brightnesses of the  $V$  galaxy images azimuthally averaged along ellipses with shape parameters derived from an isophotal analysis (the horizontal axis plots the major axis for the averaging ellipse). The solid curve shows the summed model (the sum of all three model components). (b) Dwarf lenticular galaxy SRGb 063.035, which is a close companion to NGC 80. The shape of the profile can successfully be fit with an exponential having a single characteristic scale, i.e., with a single stellar disk.

it as an S0 galaxy that is probably in the process of forming. It is striking that the tidal influence of massive neighbors has “shortened” the brightness profiles of the dwarf galaxies and stimulated their secular evolution, “smoothing” the overall stellar-density distribution into a single exponential law. This provides an interesting clue to possible origins of the typical exponential surface-brightness profiles of stellar disks, which are not fully understood.

Figure 4 compares the central surface brightnesses and scales for the exponential distributions for all three types of structural component—the outer and inner disks and the exponential bulge. The central surface brightnesses reduced to a face-on orientation are here presented; we necessarily took into account the internal absorption in the galaxies, as well as the fact that the stellar disks in the lenticular galaxies are “thick.” Historically, after the publication of the first

**Table 3.** Parameters of photometric components of galaxies in the NGC 80 group

Number	Filter	PA*	$(1 - b/a)^*$	Outer disk			Inner disk			Bulge			
				$\mu_0,$ $m/\text{arcsec}^2$	$h,$ arcsec	$h,$ kpc	$\mu_0,$ $m/\text{arcsec}^2$	$h,$ arcsec	$h,$ kpc	$n$	$\mu_0,$ $m/\text{arcsec}^2$	$h,$ arcsec	$h,$ kpc
(NGC 80)	<i>B</i>	4°	0.11	22.6	25.1	9.4	20.7	5.7	2.1	1	18.4	2.0	0.7
(NGC 80)	<i>V</i>			21.4	27.7	10.3	19.4	4.8	1.8	1	17.3	1.8	0.7
029	<i>B</i>	166	0.52	24.1	8.8	3.3	—	—	—	—	—	—	—
029	<i>V</i>			23.1	8.7	3.2	—	—	—	—	—	—	—
030	<i>B</i>	100	0.26	23.2	9.5	3.5	—	—	—	—	—	—	—
030	<i>V</i>			23.0	9.4	3.5	—	—	—	—	—	—	—
034	<i>B</i>	110	0.1	24.6	17.3	6.5	20.1	2.2	0.8	1	19.0	1.1	0.4
034	<i>V</i>			23.3	16.7	6.2	19.1	2.2	0.8	1	17.9	1.1	0.4
035	<i>B</i>	159	0.1–0.18	—	—	—	22.0	4.0	1.5	—	—	—	—
035	<i>V</i>			—	—	—	20.7	3.3	1.2	—	—	—	—
040	<i>B</i>	148	0.18	22.6	9.2	3.4	21.6	5.7	2.1	1	20.0	2.2	0.8
040	<i>V</i>			21.6	9.2	3.4	20.3	6.2	2.3	1	19.0	2.4	0.9
016	<i>B</i>	35	0.64	24.5	24.6	9.2	21.3	7.5	2.8	1	19.2	2.1	0.8
016	<i>V</i>			22.5	15.7	5.9	18.6	5.8	2.2	1	17.1	2.2	0.8
055	<i>B</i>	85	0.36	23.1	11.5	4.3	21.5	6.3	2.4	1	19.5	2.2	0.8
055	<i>V</i>			22.4	12.5	4.7	20.6	6.3	2.4	1	18.6	2.5	1.0
058	<i>B</i>	53	0.36	23.4	26.1	9.7	20.6	7.2	2.7	2	20.6	4.1	1.5
058	<i>V</i>			22.5	25.5	9.5	19.4	7.6	2.8	2	19.5	3.1	1.2
041	<i>B</i>	8	0.64	22.8	9.0	3.4	19.1	4.8	1.8	1	19.3	2.0	0.8
041	<i>V</i>			22.2	11.4	4.2	18.9	4.9	1.8	1	18.4	2.0	0.8
044	<i>V</i>	116	0.53	23.4	23.0	8.6	21.0	9.0	3.4	—	—	—	—
051	<i>B</i>	32	0.32	22.6	9.0	3.4	20.4	6.9	2.6	—	—	—	—
051	<i>V</i>			22.7	9.6	3.6	19.5	6.9	2.6	1	22.9	1.4	0.5
(UCM)	<i>B</i>	105	0.10	25.0	7.5	2.8	—	—	—	1	20.3	1.8	0.7
(UCM)	<i>V</i>			24.0	7.0	2.6	—	—	—	1	19.5	1.8	0.7

\* Orientation parameters (position angle for the major axis PA and ellipticity) refer to the outermost measured isophotes.

statistics for the parameters of stellar disks of nearby galaxies by Freeman [27], who reported that the central surface brightnesses were grouped near the value  $\mu_0(B) = 21.7^m/\text{arcsec}^2$  and had a Gaussian distribution with the width of the order of the measurement errors, virtually all subsequent photometric surveys have given broad distributions for the central surface brightnesses and a correlation between the central surface brightness and the exponential scale of the disk (see, for example, [28–31] and others). However, these surveys did not allow for the possible

presence of multi-tiered exponential disks. A correlation between the central surface brightness and the exponential scale is also obvious in our Fig. 4, where up to three structural components are superposed for each galaxy; however, we can now see that the existence of this correlation is actually due to the presence of three types of structural component with various degrees of concentration of the density toward the center. The three clouds of points corresponding to the outer disks, inner disks, and exponential bulges have various mean scales and central surface

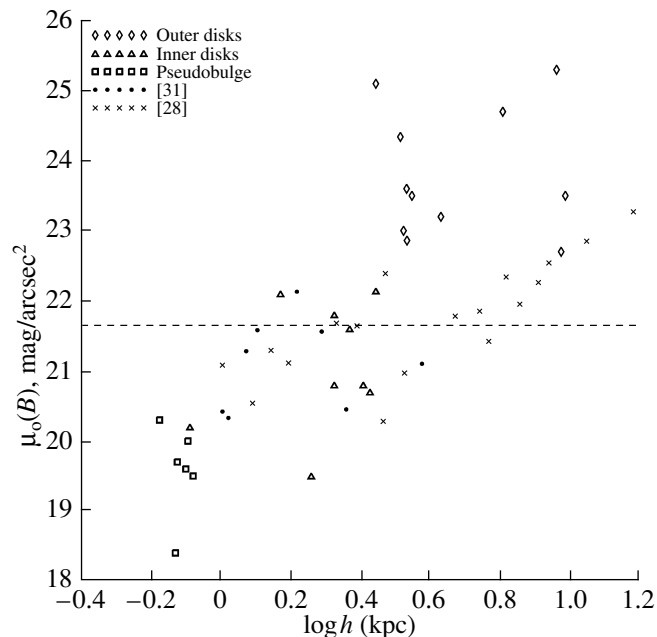


**Fig. 4.** Empirical relation between the central surface brightness and the characteristic exponential scales for the stellar disks of early-type galaxies. Our results for the outer disks, inner disks, and pseudobulges are superposed, together with literature data from photometric surveys specifying only one exponential disk in the models. The horizontal dashed line indicates the mean central surface brightness of global stellar disks of nearby galaxies according to Freeman [27].

brightnesses, but no correlation between scale and central surface brightness is observed within each cloud of points. The outer disks all have lower surface brightness than the “Freeman standard,” while the inner disks are all brighter. It is not ruled out that there is no physical correlation between scale and surface brightness, while there exist several types of stellar disks with different origins. However, this conclusion requires verification based on brightness-profile decompositions for a larger statistical sample taking into account the presence of multi-tiered disks.

In the construction of the model images for the galaxies and the subtraction of these from the observed images, apart from the large-scale structural components, it was possible in a number of cases to also distinguish small-scale peculiar structures, which are clearly visible in the residual-brightness maps in Figs. 1 and 2. We present a brief description of these substructures for each galaxy below.

**NGC 86.** The stellar population at the galactic center is old [18]. After subtracting the outer and inner exponential disks, a “boxy” bulge with spiral arms remains in the brightness distribution, with the position angle of the major axis of the bulge, about  $170^\circ$ , differing appreciably from the orientation of the disks. The best fit to the bulge is obtained using a Sérsic law with an index of one (an exponential bulge) and with  $r_0 = 2''$ ,  $\mu_0 = 19^m/\text{arcsec}^2$ , and the ratio

of the minor and major axes being about 0.95. Subtracting this bulge leads to a residual image that is reminiscent of a bar that is evolved in the  $z$  direction. The residual brightness after this subtraction occupies roughly 50% of the total area of the bulge, i.e., it is more compact. We suggest that the exponential bulge of the galaxy is a pseudobulge whose origin is associated with the development of vertical instability in a bar [32].

**NGC 85.** The outer disk begins to dominate the brightness profile at distances  $r > 20''$  (7.5 kpc) from the center, and its parameters are characteristic for the “mean” disks of spiral galaxies (Table 3). After subtracting the outer disk, the residual has an exponential profile with excess brightness near the southern edge. One has the impression that the obtained inner disk has a higher inclination and a smaller position angle than the outer disk. The new orientation parameters are  $i = 50^\circ$ ,  $\text{PA} = 137^\circ$ . Fitting an exponential to the brightness profile in the radius range  $8\text{--}15''$  yields the parameters of a second disk (Table 3). After subtracting this disk as well, the residuals resemble a small lens-like region with “tails.” It is interesting that the position angle of the small lens seems closer to the position angle of the outer than of the inner disk, whereas the opposite is true of its inclination. We have recently seen a similar structure in the counter-rotating lenticular galaxy NGC 5631, which clearly demonstrates effects of a minor merger [33]. Further fitting of the residual



brightness profile for NGC 85 seems to indicate a fairly elongated exponential bulge ( $b/a = 0.83$ ). The residuals after subtraction of this bulge visually resemble three features with tails, which are likely a consequence of a recent merger, which also led to the formation of the lenticular galaxy.

**PGC 1384.** It is immediately obvious that this galaxy contains large amounts of dust. Since the galaxy is viewed nearly edge-on, the dust strongly impedes the decomposition, as the galactic center is hidden within this dust. It is interesting that dust is not visible in the outer disk of this very dusty galaxy, which apparently testifies to secular evolution during which the gas and dust have become more concentrated toward the galactic center. Therefore, we adopted as the model nucleus the center of the outer, rather than the inner, isophotes. The fitting of the outer disk was carried out for  $r > 30''$ . At  $r < 19''$ , the residual profile in the  $V$  filter is fit well by an exponential law corresponding to a second disk. We were not able to analyze the most central region of the galaxy, since they were strongly screened by dust, even in the  $V$  filter.

**UCM 0018+2216.** The name of this galaxy indicates that it was discovered in the Universidad Complutense de Madrid survey, which was aimed at searching for emission-line galaxies. Subsequent long-slit spectroscopy [34] showed that a modest intensity of star formation is occurring in the galactic nucleus. Our images display a modest asymmetry of the galaxy relative to the center of the inner isophotes: its southeastern edge is more elongated than its northwestern edge. Because of this, the northern parts of the galaxy are slightly “oversubtracted,” and the residual brightness is shifted to the south of the center. The outer disk begins to dominate at  $r > 13''$ . After subtracting the outer disk, a second exponential disk can be fit to the residual profile at  $r = 2\text{--}6''$ . After subtracting both disks, there remains an interesting region resembling a boxy bulge with an elongated shape and a sort of weak, tightly wound spiral structure (ring?) visible in the  $B$  filter.

**IC 1548.** The stellar population in the galactic center is young: younger than 1.5 billion years in the nucleus and 3 billion years in the bulge [18]. After subtracting the two exponential disks from this fairly strongly inclined lenticular galaxy, there remains a circular exponential bulge surrounded by rudimentary spirals.

**CGCG 479-014B.** This is a late-type spiral with a large bar. The brightness profile of the outer disk has type II according to the scheme of Freeman [27]—exponential with a “hole” in the center. The bulge is small and circular, and its Sérsic parameter is determined only uncertainly due to its compactness.

**NGC 93.** Our previous study [18] revealed a chemically distinct nucleus in the old bulge of this galaxy, which formed 3–4 billion years ago in a secondary burst of star formation. The powerful dust band visible in images indicates that the northwestern part of the disk is located on the near side of the galaxy. When constructing our models, we had to mask both the region of strong dust absorption and the high-contrast spiral arms. The outer disk begins to dominate at  $r = 43''$  (16 kpc), while the inner disk dominates at  $r = 20\text{--}40''$ . After subtracting the two disks, there remains a small lens-like region that is asymmetrical due to the presence of the dust band. It is possible to fit the residual brightness at  $r = 5\text{--}11''$  using a single ring disk (with a “hole” at its center), with its brightness profile cut off at  $r > 11''$ . After fitting the residual brightness at  $r = 2\text{--}11''$  with a Sérsic bulge with  $n = 2$  and isophote ellipticity 0.75, a very interesting residual brightness distribution appears, which resembles a one-sided bar (whose other half is hidden by dust) or a satellite that is smeared by tidal forces.

**IC 1541.** The stellar population at the galactic center is old [18]. See Fig. 3a for an analysis of the surface-brightness profile. The apparent axial ratio for the exponential bulge is 0.8.

**NGC 80.** The decomposition of this galaxy agrees well in terms of scale with the results published by us earlier based on less deep data [35]. The outer regions can be fit with an exponential profile beginning at a distance of  $30''$  (11 kpc). The inner disk dominates at radii  $10\text{--}20''$  (4–7 kpc). After subtracting the two disks, the residual brightness at  $r = 2\text{--}8''$  can be fit with a circular exponential bulge. Excess brightness is visible at  $r = 5\text{--}7''$ , coincident with the location of a ring of relatively young stars ( $T \sim 5$  billion years) [35, 18].

**NGC 81.** An outer exponential disk fits the galaxy profile well at  $r > 15''$ , and an inner disk from  $6''$  to  $12''$ . After subtracting these two disks, the residual structure resembles a lens with modest spiral arms, which we fit with an exponential bulge with axial ratio  $b/a = 0.95$ . After subtracting the bulge, there remain residual tails resembling a spiral structure. The bulge apparently has boxy isophotes.

**SRGb 063.030.** The outer disk displays an exponential profile beginning at  $r = 11''$  (4 kpc). After subtraction, the residual profile has a bulging shape that cannot be fit using a Sérsic law with  $n \geq 1$ .

**SRGb 063.029.** The outer disk begins at  $15''$  (5.5 kpc). After subtracting this outer disk, the residual profile has a bell-like shape.

**SRGb 063.035.** This galaxy is very compact, and can be described by a single exponential brightness

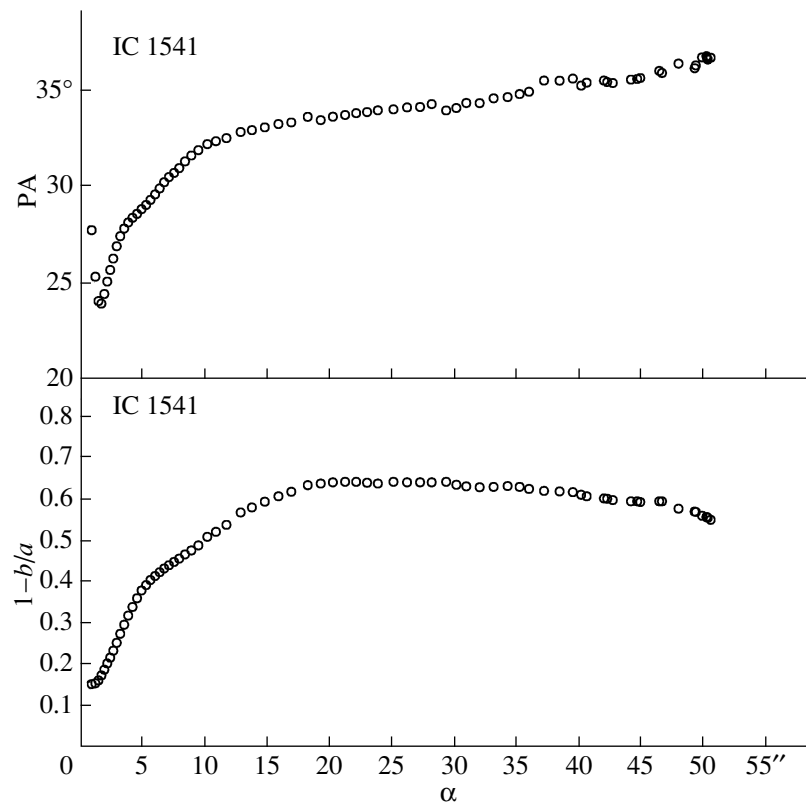


**Fig. 5.** Results of an isophotal analysis for IC 1541 (in  $V$ ): radial dependences of the position angle and ellipticity.

profile (Fig. 3b). It is most likely that its outer regions have been “ripped off” by the tidal influence of NGC 80, which is at a distance of only 20 kpc projected onto the plane of the sky.

#### 4. ROTATION CURVE OF THE LENTICULAR GALAXY IC 1541

We obtained a long-slit spectrum of IC 1541 with the slit oriented roughly along the major axis of the galaxy. We hoped to find ionized gas, but no signs of emission lines were detected in the spectrum over the entire extent of the galactic disk. However, we used this spectrum to estimate the rotational velocity of the stellar component: we were able to measure radial velocities from absorption lines to distances of roughly  $15''$  (6 kpc) from the center.

As we noted above, the surface-brightness profile of IC 1541 was decomposed into three exponential segments with different characteristic scales. Based purely on the surface photometry, the structure of the galaxy can be interpreted either as a combination of three disks, or a two-tiered disk and a pseudobulge, or an outer disk and a combined bulge. However, the stellar dynamics of the bulge and disk are different: the bulge is a dynamically hot (thick) subsystem, while the disk is a dynamically cool subsystem, where

ordered rotation dominates over random motions (the velocity dispersion) of the stars. Accordingly, we can diagnose the stellar exponential structures by comparing the observed ordered stellar motions with the predictions of a rotation model for a system with a specified geometry and density distribution that is consistent with the observed surface-brightness distribution. Here, we necessarily neglect the possible contribution of dark matter, but, as is known from statistics, as a rule, the dynamical influence of dark matter is small in the central regions of massive disk galaxies (see, for example, [36]).

We took the model for the rotation of an axially symmetrical flattened stellar system with an exponential profile for the projected surface density from [37]. This paper presents tabulated circular rotation curves for three ratios of the characteristic effective disk thickness and the characteristic effective radius (related to the characteristic exponential scale by the factor 1.678): 0.05, 0.1, and 0.2. The last of these three values corresponds to a so-called “thick” disk, which is considered to be typical for lenticular galaxies [38, 39], and IC 1541 is a lenticular galaxy. Figure 5 presents the results of an isophotal analysis for IC 1541 (in  $V$ ). Judging from the fact that the radial dependence of the isophote ellipticity has reached a plateau by radii  $10\text{--}15''$ , i.e., inside the zone

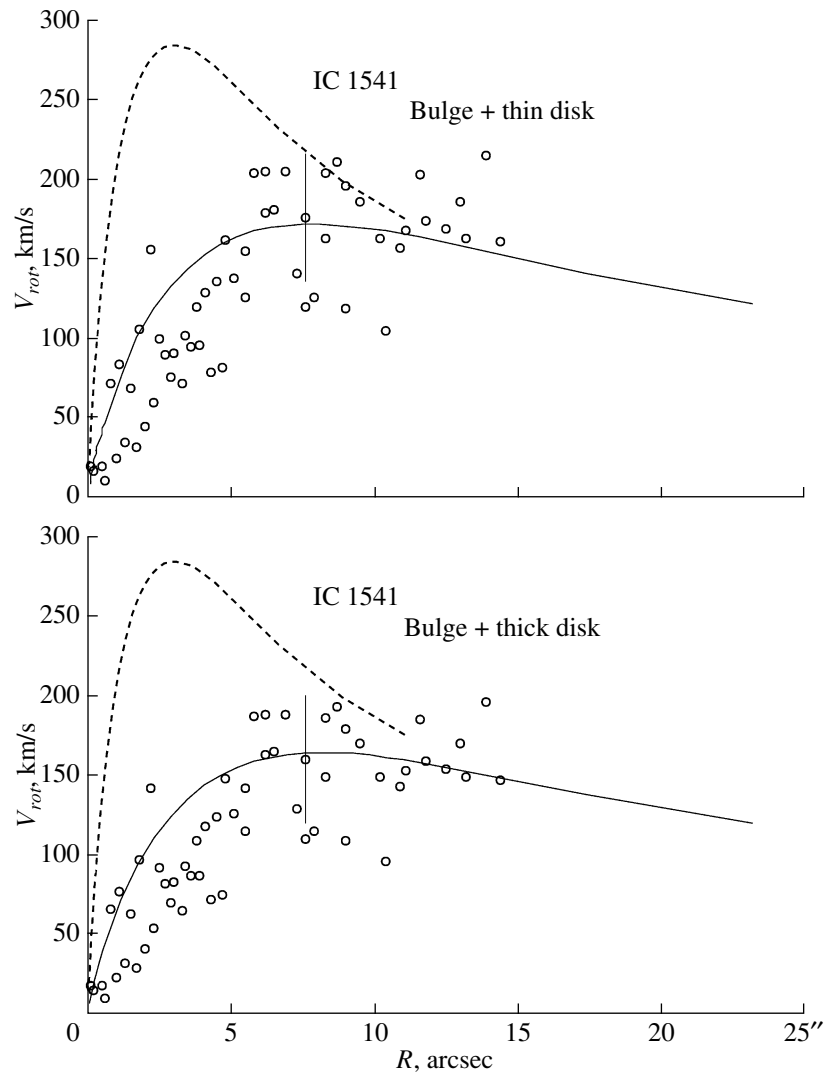


**Fig. 6.** Rotation curve for the stellar component of IC 1541. The circles show the observational data (SCORPIO), the solid curve the dynamical model for the inner disk (a middle exponential component with parameters derived from surface photometry and for two assumptions about the disk thickness, see text for details), and the dashed curve the dynamical model for the most central exponential component assuming that it could be a thick disk. The typical measurement error is indicated by the vertical line shown for one of the observational data points.

of photometric dominance of the middle exponential component (Fig. 3a), the two outer components have comparable thicknesses, and are most likely disks. The inner exponential component could be either a disk or a bulge. Figure 6 compares the observed rotational velocities for the stellar component of IC 1541 and models from [37] for two types of middle disk—“thin” (ratio of the vertical to the radial scales 0.05) and “thick” (ratio of the vertical to the radial scales 0.2); we always consider the inner exponential component to be a “thick” disk. Based on the isophotal analysis of Fig. 5 and the guidelines given in [39], according to which, for disks of finite thickness,  $\sin i = \sqrt{\frac{2e-e^2}{1-q_0^2}}$ , where  $e \equiv (1 - b/a)$  is the

apparent ellipticity of the isophotes and  $q_0$  the true ratio of the vertical to the radial scales, we specify for the “thin” disk a viewing angle of  $67^\circ$ , while the “thick” disk is viewed edge-on. We took  $M/L_V = 3.8$  for the mass-to-light ratio required to recalculate the surface-brightness profile to a surface density profile, from the stellar-population models of [40] for a metallicity of +0.25 and an age of 5 billion years. Figure 6 shows that both models can satisfactorily describe the observational data for radii 5–15'' (the “thick disk” model may be slightly better). Inside a radius of 5'', where the innermost exponential component dominates photometrically, there is an obvious divergence of the model from the observations. This is due to the fact that the asymmetric drift has not

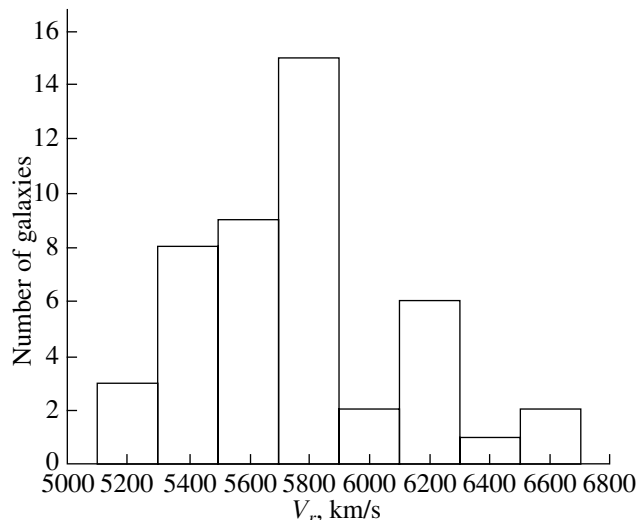


**Fig. 7.** Histogram of the distribution of galaxy radial velocities in the NGC 80 group according to the data of [19]. The systemic velocity of the group and the radial velocity of the central galaxy, NGC 80, are about 5700 km/s.

been taken into account (the velocity dispersion at the center of IC 1541 reaches 140 km/s), and also possibly because the innermost component is not a dynamically cool disk, and its relative thickness is much greater than 0.2. As expected, the influence of dark matter is negligible at the center of IC 1541.

Thus, we conclude based on a comparison of the model rotation curve and the observed radial velocities for the stellar component of IC 1541, that the innermost exponential stellar component is a bulge, while the middle component is a disk with a thickness that is typical for lenticular galaxies.

## 5. MINOR MERGER OF THE LENTICULAR GALAXY NGC 85

In our previous paper [18], dedicated to the characteristics of the stellar populations in the centers of large galaxies of the NGC 80 group, we suggested that the subgroup of the giant elliptical galaxy NGC 83 is currently accreting onto the NGC 80 group. We were led to this idea by the large difference in the radial velocities of NGC 83 and the dynamical center of the group (next to which it is projected),  $\sim 500$  km/s, and the appreciable ongoing star formation in the center of this giant elliptical galaxy. Further studies whose results we publishing now have supported our earlier suspicions about this.

Figure 7 shows a histogram of the distribution of galactic radial velocities in the region of the NGC 80 group measured in [19] for 45 objects within  $\pm 1000$  km/s and within 1.5 Mpc from the center of the group. Although this distribution can formally be

fit with a Gaussian corresponding to a velocity dispersion of 300 km/s, as is normal for massive X-ray galaxy groups, there is a concentration of  $\sim 10$  objects near the velocity of NGC 83 ( $\sim 6200$  km/s). Excluding these objects from the NGC 80 group reduces the estimated velocity dispersion for the remaining galaxies to 224 km/s. The histogram in Fig. 7 on its own does not enable us to distinguish the NGC 83 subgroup in a statistically significant way; however, we can note certain common properties of the galaxies concentrated near the velocity of NGC 83. First, these are also concentrated spatially around NGC 83: most of them are located to the North of NGC 80. Second, virtually all of these galaxies display ongoing or recent star formation, beginning with NGC 83 itself. In addition to NGC 83, SRG 063.023 is a Markarian galaxy (Mrk 1142) indicating that it's nucleus has ultraviolet excess in the spectrum. The giant spiral galaxy MGC + 04 – 02 – 010 appears in the Madrid survey of emission-line galaxies as UCM 0018+2218 [41], and is spectrally classified as a starburst galaxy (SBN) in [34]. Finally, the lenticular galaxy NGC 85, which is near NGC 83 in terms of both its velocity and its spatial location, and which was studied by us using the MPFS spectrograph, also proves to be unusually “young.”

Figure 8 presents a diagnostic diagram comparing the  $H\beta$  and  $[MgFe] \equiv \sqrt{Mg b \langle Fe \rangle}$  Lick indices for the galaxies NGC 83 and NGC 85 obtained with the MPFS and models of “simple” stellar populations of Thomas et al. [24]. This comparison can be used to distinguish the effects of age and metallicity, and to

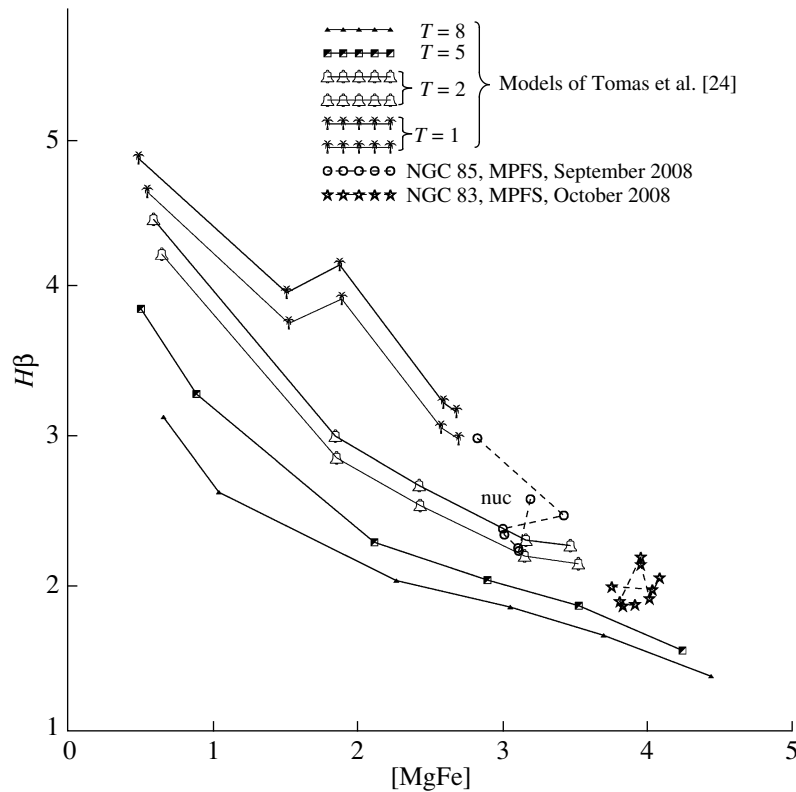


**Fig. 8.** Diagnostic diagram for determining the mean age and metallicity of a stellar population based on the Lick indices. Our observational data for the central regions of the galaxies NGC 83 [18] and NGC 85 (this paper) obtained with the MPFS are shown, together with models for “simple” stellar populations of Thomas et al. [24]. The model ages  $T$  are given in billions of years; the model metallicities for the symbols joined by solid curves are, from right to left, +0.67, +0.35, 0.00, −0.33, −1.35, and −2.25 (in the case of six points). Azimuthally averaged observational data for the galaxies were obtained in steps of 1'' in radius and are joined by the dashed curve in order of increasing  $R$ ; the nucleus is denoted “nuc.”

determine mean values of both of these characteristics for a stellar population (weighted according to luminosity). The diagram in Fig. 8 clearly demonstrates that, like NGC 83, NGC 85 has fairly young stars at its center, whose mean ages are about two to three billion years in the nucleus and in a ring with a radius of 5–6'', and about five billion years in the bulge surrounding the nucleus. Obviously, the ages of the bursts of star formation in the centers of NGC 85 and NGC 83 are comparable, supporting the idea that these two galaxies share a common fate and are both intruders into the NGC 80 group. In contrast to NGC 83, NGC 85 contains no nuclear ionized gas, indicating that star formation has already ceased in its center. We can identify a likely origin for this burst of star formation: a close inspection indicates that the galaxy is interacting. The residual-brightness distribution (Fig. 1) clearly shows tidal arms, which are gravitationally being pulled out of NGC 85, one long and the opposite one short. Which of the neighbors could be the “perturber”? To the East of NGC 85 is the large spiral galaxy IC 1546, but the difference in

the radial velocities of these two galaxies is 300 km/s, and such a fast passage would not be able to facilitate the development of tidal structures. A dense, round spheroidal companion is visible to the South of NGC 85; could this be the galaxy “tugging” the arms from its neighbor? Our analysis of the distribution of the  $B - V$  color index for the “residual” field (Fig. 9) enables us to reject this hypothesis: the compact object to the South of NGC 85 has an anomalously red color for nearby dwarf galaxies,  $B - V = 1.4$ , and is most likely a background galaxy. However, a “dense condensation” at the end of the long tidal arm has an appropriate color,  $B - V = 1.1$ . This appears to be a half-disrupted satellite of NGC 85, whose accretion onto the latter gave birth to the observed tidal arms. This lenticular galaxy recently underwent a minor merger, which probably also produced the nuclear burst of star formation. The bases of the tidal arms are very blue,  $B - V \approx 0.6$ , and it is not ruled out that star formation is ongoing. If so, this indicates that there was quite recently a large amount of gas in the extended disk of the galaxy, consistent with the

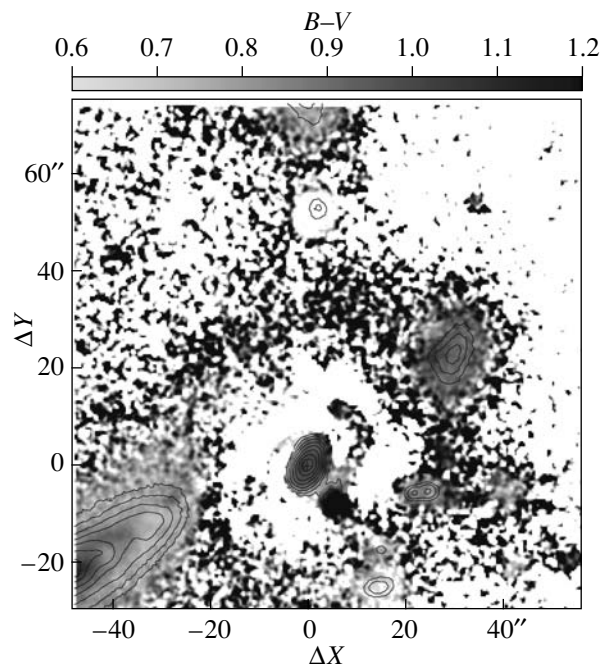


**Fig. 9.** Map of  $B - V$  for part of the group around the galaxy NGC 85 after subtracting the outer disk of NGC 85. Darker shades of gray correspond to redder colors. The isophotes show the residual  $V$  surface brightness.

possibility that NGC 85, now a lenticular galaxy, was recently a spiral. We conclude that we are observing in real time the birth of a lenticular galaxy from a spiral, and, although this is occurring within the X-ray halo of the group, the mechanism forming the S0 galaxy is, in this case, clearly gravitational and not gas-dynamical.

## 6. CONCLUSION

According to modern concepts, lenticular galaxies form from spirals and acquire their final morphology in small groups, subsequently accreting into clusters where they are currently the dominant population, together with their groups (see, for example, [3]). However, the specific mechanism bringing about this transformation has not been clear: many possible physical mechanisms capable on a time scale of only one to four billion years of removing gas from the disk of a spiral galaxy, bringing an end to star formation, and dynamically “heating” the disk, thereby suppressing spiral structure, have been proposed. These can be divided into “gravitational” mechanisms, associated with the interaction of forming S0 galaxies with other galaxies and with the overall gravitational potential of the group, and “gas-dynamical” mechanisms, associated with the interaction of cool gas of the galactic disk and hot intergalactic gas. The characteristics of the NGC 80 group, which is massive, rich, and has a hot X-ray gaseous halo, make it an ideal place for the formation of lenticular galaxies

for any plausible transformation mechanism. Indeed, a close inspection of the group reveals a substantial population of lenticular galaxies: although rich X-ray groups are thought to be primarily a location for early-type galaxies, there are only three elliptical galaxies among the several dozen members, and in one of them—NGC 83—we found earlier signs of a massive disk and intense current star formation. In the current study, we have investigated the structures of 13 galaxies selected from the largest group members. According to their literature classifications (Table 1), four of these are lenticular; however, a detailed examination of the fine structure of their stellar disks suggests that nine are actually lenticular (or, in this context, non-spiral).

Our decomposition of the radial surface-brightness profiles into components has shown that most of the lenticular galaxies in the NGC 80 group have two-tiered, exponential stellar disks and compact bulges in their centers, also with exponential brightness profiles (which are now usually referred to as “pseudobulges”). This type of structure is characteristic of both galaxies near the center of the group, including the central giant galaxy NGC 80, and galaxies at the periphery, located more than 0.5 Mpc from the group center. We do not see any systematic variation in the structure of the disk galaxies from the periphery to the center of the group, which would have suggested the transformation of spiral into lenticular galaxies in the course of their accretion onto the group

and immersion “deeper” in the X-ray halo. The only environmental effect for which there is evidence is that four dwarf S0 galaxies ( $M_B > -18$ ) with single-tiered, exponential stellar disks are close companions to the giant galaxies NGC 80 and NGC 86. Thus, it appears that the classical structure of a lenticular galaxy, with a *single* exponential stellar disk, is obtained as a consequence of the tidal stripping of the outer parts of small galaxies.

One of the large lenticular galaxies, NGC 85, shows signs of recent stimulated star formation: the mean age of the stars in its center is about two billion years, and subtracting a model for the large stellar disk reveals the presence of spiral arms with blue ends (at the center) that are clearly tidal in origin. It is possible that we are observing here the recent transformation of a spiral into a lenticular galaxy, accompanied by a burst of star formation in the galactic center one to two billion years ago. NGC 85 is located not far from the center of the group, but, according to its radial velocity, it is associated with NGC 83, and apparently joined the NGC 80 group only recently, together with NGC 83. The remnants of another smaller galaxy can be distinguished at the end of a long tidal arm, whose gravitation probably brought about the metamorphosis of NGC 85. All this supports the idea that the mechanism for the transformation of spiral into lenticular galaxies could be minor mergers. The properties of NGC 85 and the presence of well formed lenticular galaxies such as IC 1541, IC 1548, and NGC 94 [42] at the group periphery, outside the X-ray halo, seems to us to provide convincing arguments that the dominant mechanism for the transformation of spiral into lenticular galaxies in groups is gravitational, rather than gas-dynamical interaction with hot, intergalactic gas.

#### ACKNOWLEDGMENTS

The data analyzed here were obtained on the 6-m telescope of the Special Astrophysical Observatory of the Russian Academy of Sciences, which is financed by the Ministry of Education and Science of the Russian Federation (registration number 01-43). We thank A.A. Smirnova for facilitating the MPFS observations. Our analysis made use of the Lyon–Meudon Extragalactic Database (LEDa), which is maintained by the LEDa team at the Lyon Observatory CRAL (France), and the NASA/IPAC Extragalactic Database (NED), which is managed by the Jet Propulsion Laboratory of the California Institute of Technology by contract to the NASA (USA). This work was supported by the Russian Foundation for Basic Research (project code 07-02-00229a).

#### REFERENCES

1. E. Hubble, *Realm of the Nebula* (New Haven: Yale Univ. Press, 1936).
2. G. Fasano, B. M. Poggianti, W. J. Couch, et al., *Astrophys. J.* **542**, 673 (2000).
3. D. J. Wilman, A. Oemler, Jr., J. S. Mulchaey, et al., *Astrophys. J.* **692**, 298 (2009).
4. D. Burstein, *Astrophys. J.* **234**, 435 (1979).
5. C. Möllenhoff and J. Heidt, *Astron. and Astrophys.* **368**, 16 (2001).
6. V. Quilis, B. Moore, and R. Bower, *Science* **288**, 1617 (2000).
7. A. V. Zasov, *Pisma Astron. J.* **4**, 487 (1978).
8. G. Byrd and M. Valtonen, *Astrophys. J.* **350**, 89 (1990).
9. B. Moore, N. Katz, G. Lake, et al., *Nature* **379**, 613 (1996).
10. B. Moore, G. Lake, T. Quinn, and J. Stadel, *Monthly Not. Roy. Astron. Soc.* **304**, 465 (1999).
11. A. Oemler, *Astrophys. J.* **194**, 1 (1974).
12. A. Dressler, *Astrophys. J.* **236**, 351 (1980).
13. H. R. Butcher and A. Oemler, *Astrophys. J.* **226**, 559 (1978).
14. M. J. Geller and J. P. Huchra, *Astrophys. J. Suppl. Ser.* **52**, 61 (1983).
15. A. Mahdavi, H. Bohringer, M. J. Geller, and M. Ramella, *Astrophys. J.* **534**, 114 (2000).
16. M. Ramella, M. J. Geller, A. Pisani, and L. N. da Costa, *Astron. J.* **123**, 2976 (2002).
17. R. A. White, M. Bliton, S. P. Bhavsar, et al., *Astron. J.* **118**, 2014 (1999).
18. O. K. Sil’chenko and V. L. Afanasiev, *Astron. J.* **85**, 972 (2008).
19. A. Mahdavi and M. J. Geller, *Astrophys. J.* **607**, 202 (2004).
20. V. L. Afanasiev and A. V. Moiseev, *Astron. Letters* **31**, 194 (2005).
21. P. Poulain, *Astron. and Astrophys. Suppl. Ser.* **72**, 215 (1988).
22. V. L. Afanasiev, S. N. Dodonov, and A. V. Moiseev, in *Stellar dynamics: from classic to modern*, Proc. Conf., St.-Petersburg, Ed. by L. P. Osipkov, I. I. Niki-forov (Saint-Petersburg Univ. Press, 2001), p. 103.
23. G. Worthey, S. M. Faber, J. J. González, and D. Burstein, *Astrophys. J. Suppl. Ser.* **94**, 687 (1994).
24. D. Thomas, C. Maraston, and R. Bender, *Monthly Not. Roy. Astron. Soc.* **339**, 897 (2003).
25. A. V. Moiseev, J. R. Valdés, and V. H. Chavushyan, *Astron. and Astrophys.*, **421**, 433 (2004).
26. J. L. Sérsic, *Atlas de Galaxies Australes* (Cordoba, Observatorio Astronomico, 1969).
27. K. C. Freeman, *Astrophys. J.* **160**, 767 (1970).
28. R. S. de Jong, *Astron. and Astrophys.* **313**, 45 (1996).
29. E. Iodice, M. D’Onofrio, and M. Capaccioli, *Astrophys. and Space Sci.* **276**, 869 (2001).
30. A. W. Graham and W. J. G. de Blok, *Astrophys. J.* **556**, 177 (2001).

31. M. D'Onofrio, *Monthly Not. Roy. Astron. Soc.* **326**, 1517 (2001).
32. M. Bureau, G. Aronica, E. Athanassoula, et al., *Monthly Not. Roy. Astron. Soc.* **370**, 753 (2006).
33. O. K. Sil'chenko, A. V. Moiseev, and V. L. Afanasiev, *Astrophys. J.* **694**, 1550 (2009).
34. J. Gallego, J. Zamorano, M. Rego, et al., *Astron. and Astrophys. Suppl. Ser.* **120**, 323 (1996).
35. O. K. Sil'chenko, S. E. Kuposov, V. V. Vlasyuk, and O. I. Spiridonova, *Astron. J.* **80**, 107 (2003).
36. S. A. Kassin, R. S. de Jong, and B. J. Weiner, *Astrophys. J.* **643**, 804 (2006).
37. G. Monnet and F. Simien, *Astron. and Astrophys.* **56**, 173 (1977).
38. G. de Vaucouleurs, A. de Vaucouleurs, H. G. Corwin, Jr., et al., *Third Reference Catalogue of Bright Galaxies. Volume I: Explanations and References* (New York: Springer, 1991).
39. E. Neistein, D. Maoz, H.-W. Rix, and J. L. Tonry, *Astron. J.* **117**, 2666 (1999).
40. G. Worthey, *Astrophys. J. Suppl. Ser.* **95**, 107 (1994).
41. J. Zamorano, M. Rego, J. Gallego, et al., *Astrophys. J. Suppl. Ser.* **95**, 387 (1994).
42. A. T. Kalloghlian and E. H. Nikoghossian, *Astrophysics* **36**, 193 (1993).

*Translated by D. Gabuzda*